Amplified electrochemical detection of DNA through the aggregation of Au nanoparticles on electrodes and the incorporation of methylene blue into the DNA-crosslinked structure†

Di Li, Yiming Yan, Agnieszka Wieckowska and Itamar Willner*

Received (in Cambridge, UK) 29th March 2007, Accepted 10th July 2007
First published as an Advance Article on the web 2nd August 2007
DOI: 10.1039/b704731b

The amplified electrochemical sensing of DNA is accomplished by the analyte-induced aggregation of nucleic acid-functionalized Au nanoparticles, deposition of the aggregates on a thiolated monolayer-functionalized electrode, and the voltammetric analysis of the redox-active methylene blue intercalated in the nucleic acid duplexes associated with the aggregates.

The sensitive detection of DNA is of general interest for the analysis of pathogens, single-base mismatches, tissue matching, environmental analyses, and forensic applications.[1] Different electrochemical DNA sensors for the amplified analysis of DNA have been developed.[2] Enzymes,[3] metal or semiconductor nanoparticles,[4,5] or vesicles[6] have been widely employed as labels for the detection of DNA. The incorporation of redox-active units into double-stranded DNA that is formed on electrode surfaces by polymerase-induced replication of the duplex, followed by the activation of a redox enzyme by the incorporated relay has been reported as a two-step amplification for DNA analysis.[7] The aggregation of Au nanoparticles (NPs) has been used for the optical[8] and microgravimetric analysis[9] of DNA. The color changes (red to blue transformation) of nucleic acid-functionalized Au NPs as a result of hybridization with the complementary DNA, aggregation of the NPs, and the stimulation of a coupled inter-particle plasmon excitations has been used for the optical detection of DNA.[8] The layer-by-layer deposition of Au NP aggregates on piezoelectric crystals through the bridging of the layers by hybridization with the analyte DNA has been used for the amplified microgravimetric analysis of DNA.[9] In the present study we report on a new method for the amplified electrochemical detection of DNA by the assembly of Au NP aggregates on electrode surfaces and the incorporation of methylene blue, MB^+, as a redox-active intercalator into the double-stranded DNA. The crosslinked Au NP aggregates provide a conductive matrix for the activation of the electrochemical response of the incorporated MB^+, and this enables the electrochemical readout for the analysis of the DNA. The specificity of association of MB^+ to the double-stranded DNA leads to a specific DNA sensor.

Scheme 1 outlines the principle of the sensing method: Two kinds of Au NPs, each modified with the nucleic acids **1** or **2**, complementary to the 5′ or 3′ ends of the analyte DNA, **3**, are interacted with the analyzed DNA samples. In the presence of **3**, the aggregation of the NPs occurs. Subsequently, the aggregated NPs are centrifuged, dissolved in a small volume of buffer solution, and interacted with the dithiol (1,9-nonanedithiol)-functionalized Au electrode. The resulting electrode is treated with methylene blue, and the electrical response of the resulting aggregated NPs assembly is monitored. The nucleic acid-functionalized Au NPs were prepared by the modification of citrate-stabilized Au NPs (12 ± 1 nm) with the thiolated nucleic acids **1** or **2**. Spectroscopic analysis of the resulting NPs indicated an average surface coverage of *ca.* 30–40 nucleic acids per particle. Microgravimetric quartz crystal microbalance experiments indicated that the surface coverage of the dithiol monolayer corresponded to 6.25×10^{-10} mol cm^{-2}. The association of the mixture of the **1**- and **2**-functionalized Au NPs to the monolayer, at a bulk concentration of 6×10^{-9} M each, resulted in a surface coverage of the Au NPs that corresponded to 1.7×10^9 particles cm^{-2}.

Fig. 1(A) shows the differential pulse voltammograms (DPVs) of the bound MB^+ at different time-intervals of aggregation of the NPs upon analyzing 1×10^{-9} M of the DNA **3**. As the time-intervals for the aggregation of the Au NPs is prolonged, the voltammetric responses of the MB^+ are intensified, and they level

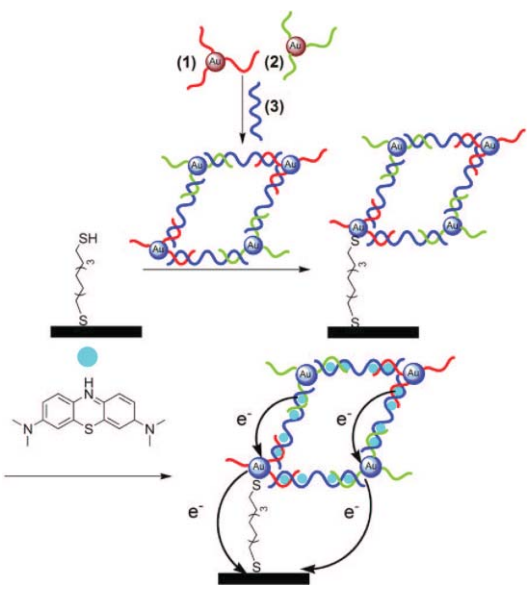

Scheme 1 Electrochemical detection of DNA through the aggregation of Au NPs and the voltammetric response of the redox-active MB^+ intercalator in the duplex-aggregated NPs. (**1**) = 5′-SH-$(CH_2)_6$-GCGCGAACCGTATA-3′ (**2**) = 5′-TCTATCCTACGCT-$(CH_2)_6$-SH-3′ (**3**) = 5′-AGCGTAGGATAGATATACGGTTCGCGC-3′.

Institute of Chemistry, The Hebrew University of Jerusalem, Jerusalem 91904, Israel. E-mail: willnea@vms.huji.ac.il; Fax: +972 2 6527715; Tel: +972 2 6585272

† Electronic supplementary information (ESI) available: experimental section and QCM results. See DOI: 10.1039/b704731b

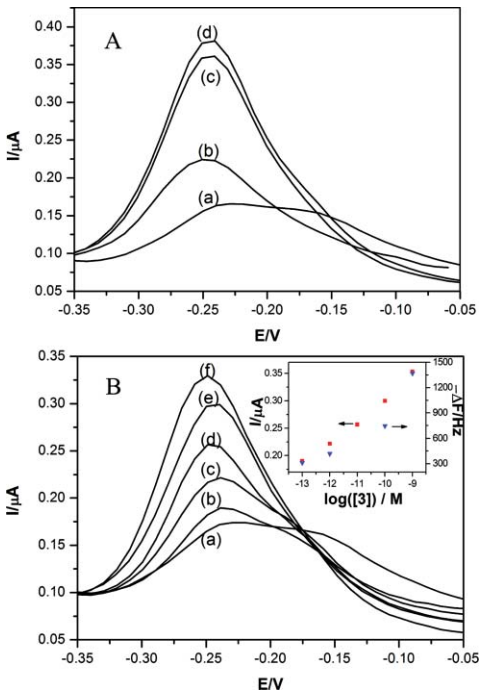

Fig. 1 (A) Differential pulse voltammograms corresponding to the responses of the MB^+ intercalated into Au NP aggregates generated in the presence of **3**, 1×10^{-9} M, at different time intervals: (a) 0 min, (b) 5 min, (c) 10 min, (d) 20 min. (B) Differential pulse voltammograms corresponding to the analysis of different concentrations of **3** according to Scheme 1: (a) 0 M, (b) 1×10^{-13} M, (c) 1×10^{-12} M, (d) 1×10^{-11} M, (e) 1×10^{-10} M, (f) 1×10^{-9} M. Inset: ■ derived calibration curve from DPV results; ▼ derived calibration curve from QCM results. In all experiments the concentration of the probing **1**- and **2**-functionalized Au NPs was 6×10^{-9} M, and the aggregation time interval prior to the deposition of the aggregates on the electrode surfaces was 20 min.

off to a saturation value after *ca.* 20 min of aggregation. It should be noted that at $t = 0$ the voltammetric response, Fig. 1(A), curve (a) shows two weak waves that correspond to the interaction of MB^+ with non-aggregated **1**- and **2**- functionlized Au NPs, $E = -0.25$ V, and to the non-specific adsorbed MB^+ to the Au electrode, $E = -0.15$ V.[10] These results are consistent with the fact that a higher degree of aggregation by the crosslinking DNA units **3** results in higher content of the MB^+ that intercalates only into the duplex structures. Furthermore, the results indicate that the Au NP aggregates provide conductive matrices that enable the electrochemical activation of the MB^+ intercalated within the growing Au NP aggregates. Accordingly, an aggregation time-interval of 20 min was selected to probe different concentrations of the analyte DNA, **3**. Fig. 1(B) shows the DPVs recorded upon analysing different concentrations of **3**. Fig. 1(B), curve (a) depicts the DPV resulting upon the treatment of the dithiol-functionalized electrode in the absence of any analyte. The **1**- and **2**-functionalized Au NPs associate with the dithiol monolayer (*vide supra*). The low DPV response may be attributed to minute non-specific or electrostatic adsorption of MB^+ to the negatively charged surface. The derived calibration curve is shown in Fig. 1(B), inset. The detection limit for analyzing **3** is estimated to be 1×10^{-13} M. Table 1 summarizes the detection limits reported for different DNA sensors. The comparison indicates that the present method reveals an enhanced sensitivity as compared to optical or electrochemical protocols that involve metallic NPs as labels. Only the scanometric method[12] or the microgravimetric quartz crystal microbalance method[15] reveal better sensitivities. The need, however, of a secondary chemical reaction of metal deposition or metallic NP catalytic labels in the latter two methods introduces increased complexity. The formation of Au NP aggregates bridged by the analyte **3** is further supported by microgravimetric QCM experiments that enabled to follow the frequency changes of the crystal as a result of aggregation of the NPs at different concentrations of the analyte, Fig. 1(B), inset. The coverage of the Au NPs upon analysing 1×10^{-9} M of **3** is *ca.* 4-fold higher than the maximum coverage of the non-bridged Au NPs linked to the electrode. Furthermore, even at the concentration of 1×10^{-13} M of **3**, the coverage of the Au NPs is *ca.* 10% higher than the surface coverage of the unbridged Au NPs. It should be noted that at the low concetration of **3** most of the generated aggregates are in a dimer configuration. The QCM results suggested that these dimer NP aggregates on the surface are at a coverage significantly higher than their statistical formation in the solution. Although the origin of this observation is at present not fully understood, the higher stabilities of dimer binding to the thiolated monolayer[16] and the displacement of individual particles might cause the elevated coverage of the dimers on the surface.

The sensing method reveals specificity. Fig. 2, curve (a) shows the DPV corresponding to the analysis of the fully complementary analyte DNA, 1×10^{-9} M, whereas Fig. 2, curves (b) and (c) depict the DPVs observed upon analyzing the single-base mutants

Table 1 Comparison of sensitivity limits of different DNA sensors

Assay	ss DNA	Ref.
Colorimetric (Au NPs)	~10 nM	8
Electrochemical (Au NPs aggregation)	0.1 pM	present study
Electrochemical (redox intercalator)	0.4 pM	11
Electrochemical (nanoparticles)	0.3 nM	4
Scanometric (Au NPs with Ag amplification)	50 fM	12
Electrochemical (liposome labels)	50 fM	13
Fluorescence (CdSe/ZnS quantum dots)	2 nM	14
Quartz crystal microbalance (Au NPs)	~1 fM	15

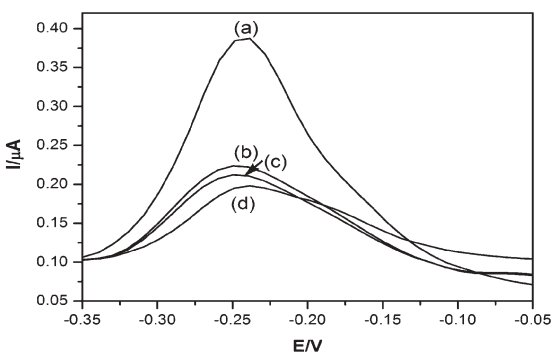

Fig. 2 Differential pulse voltammograms corresponding to the analysis of **3**, curve (a), and of the single-base mismatch **3a** (5′-AGCGTAGGATAGATATACG***C***TTCGCGC-3′), curve (b), **3b** (5′-AGC***C***TAGGATAGATATACGGTTCGCGC-3′), curve (c) and the two-base mismatch, **3c**, (5′-AGC***C***TAGGATAGATATACG***C***TTCGCGC-3′), curve (d), according to Scheme 1. In all experiments the concentration of **3**, **3a**, **3b** and **3c** was 1×10^{-9} M. All other conditions are given in Fig. 1.

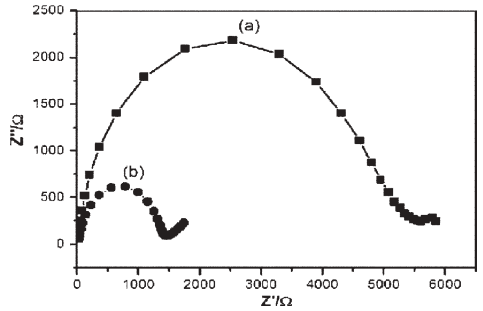

Fig. 3 Faradaic impedance spectra corresponding to (a) the Au NP aggregates generated in the presence of **3**, 1×10^{-9} M, (20 min of aggregation) and subsequent deposition on the electrode, (b) The Au NPs associated on the surface in the absence of the cross-linking **3** unit. In all experiments the concentration of the **1**- and **2**-modified Au NPs was 6×10^{-9} M, the concentration of the $Fe(CN)_6^{3-/4-}$ was 10 mM. Measurements were performed at $E = 0.2$ V, and using the 5 mV alternative voltage in the frequency range of 100 mHz to 10 kHz.

3a and **3b** at a concentration of 1×10^{-9} M. These mutants include a single-base mismatch in respect of the **1**- or **2**-functionalized Au NPs. Clearly, the voltammetric responses are substantially lower. Thus, the presence of the mutation site perturbs the hybridization with the respective Au NPs, and the aggregation is hindered. Hence, the voltammetric response originates from the association of a single-type of Au NP that includes an intact duplex that binds MB^+ or to a perturbed aggregate structure that binds MB^+. Fig. 2, curve (d), includes two mutations at the domains that bind to the two kinds of the Au NPs. A lower intensity of the DPV is observed as compared to the DPV obtained for **3a**. This is consistent with the fact that the two mutation sites inhibit the aggregation process, and thus, the electrochemical response of MB^+ is low.

Further support that Au NP aggregates are formed on the dithiol-modified Au surface upon the analysis of the DNA is obtained from Faradaic impedance measurements and SEM imaging of the surfaces. Fig. 3 shows the Faradaic impedance spectra (in the form of Nyquist plots) corresponding to the nucleic acid-functionalized Au NPs accumulated on the surface in the presence of the **3**-aggregated Au NPs, curve (a) and in the absence of the DNA **3**, curve (b). In these experiments no MB^+ is intercalated into the systems, and $Fe(CN)_6^{3-/4-}$ is used as a diffusional redox label. The interfacial electron transfer resistance in the presence of the **3**-aggregated NPs, $R_{et} = 5.4$ kΩ is higher than the interfacial electron transfer resistance observed with the Au NP that accumulated on the surface in the absence of **3**, $R_{et} = 1.4$ kΩ. These results agree well with the fact that the **3**-aggregated Au NPs are highly charged by the nucleic acid modifying units, and these electrostatically repel the negatively charged redox label, thus introducing a barrier for electron transfer to the redox probe.

The SEM images of the dithiolated-monolayer-functionalized Au surface treated with the **1**- and **2**-functionalized Au NPs in the absence of **3** or after hybridization with **3** are shown in Fig. 4(A) and (B), respectively. Clearly, in the absence of **3**, only individual NPs are observed, while in the presence of **3**, aggregates of the Au NPs are observed, and these originate from the crosslinking of the Au NPs through hybridization of **3**.

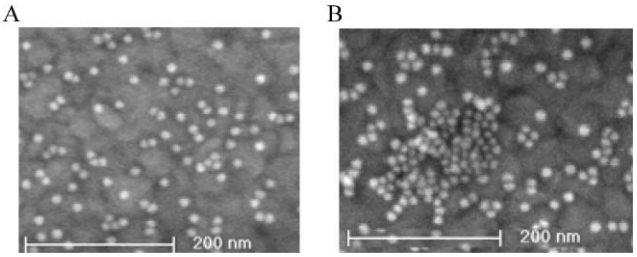

Fig. 4 SEM images of: (A) The Au NPs deposited on the thiolated Au surface in the absence of the cross-linker **3**. (B) The Au NP aggregates deposited on the thiolated Au surface where the aggregates were generated in the presence of **3**, 1×10^{-9} M, for a time-interval of 20 min.

In conclusion, the present study has demonstrated a new sensitive method for the electrochemical detection of DNA. The method is based on the aggregation of Au NPs by the analyte DNA, the deposition of the aggregated NPs on a thiolated monolayer on a Au electrode, and the readout of the aggregated NPs by the electrochemical response of MB^+ intercalated in the duplexes that bridge the Au aggregates. While the MB^+ units provide a specific electrochemical indicator for the formation of the duplex DNA structures, the Au NP aggregates provide the electrical contact of the intercalated MB^+ with the electrode.

This research is supported by the Israel Ministry of Science and by the Israel Ministry of Defense.

Notes and references

1 R. F. Service, *Science*, 1998, **282**, 399–401; E. K. Lobenhofer, P. R. Bushel, C. A. Afshari and H. K. Hamadeh, *Environ. Health Perspect.*, 2001, **109**, 881–891; J. M. Butler, *J. Forensic Sci.*, 2006, **51**, 253–265; K. M. Kurian, C. J. Watson and A. H. Wyllie, *J. Pathol.*, 1999, **187**, 267–271.
2 J. J. Gooding, *Electroanalysis*, 2002, **14**, 1149–1156; T. G. Drummond, M. G. Hill and J. K. Barton, *Nat. Biotechnol.*, 2003, **21**, 1192–1199; S. O. Kelley, E. M. Boon, J. K. Barton, N. M. Jackson and M. G. Hill, *Nucleic Acids Res.*, 1999, **27**, 4830–4837.
3 L. Alfonta, A. K. Singh and I. Willner, *Anal. Chem.*, 2001, **73**, 91–102.
4 J. Wang, G. Liu and A. Merkoçi, *J. Am. Chem. Soc.*, 2003, **125**, 3214–3215.
5 J. Wang, G. Liu, R. Polsky and A. Merkoçi, *Electrochem. Commun.*, 2002, **4**, 722–726.
6 F. Patolsky, A. Lichtenstein and I. Willner, *Chem.–Eur. J.*, 2003, **9**, 1137–1145; F. Patolsky, A. Lichtenstein and I. Willner, *J. Am. Chem. Soc.*, 2000, **122**, 418–419.
7 F. Patolsky, Y. Weizmann and I. Willner, *J. Am. Chem. Soc.*, 2002, **124**, 770–772.
8 N. L. Rosi and C. A. Mirkin, *Chem. Rev.*, 2005, **105**, 1547–1562; R. Elghanian, J. J. Storhoff, R. C. Mucic, R. L. Letsinger and C. A. Mirkin, *Science*, 1997, **277**, 1078–1081.
9 F. Patolsky, K. T. Ranjit, A. Lichtenstein and I. Willner, *Chem. Commun.*, 2000, 1025–1026.
10 E. L. S. Wong, P. Erohkin and J. J. Gooding, *Electrochem. Commun.*, 2004, **6**, 648–654.
11 M. R. Gore, V. A. Szalai, P. A. Ropp, I. V. Yang, J. S. Silverman and H. H. Thorp, *Anal. Chem.*, 2003, **75**, 6586–6592.
12 T. A. Taton, C. A. Mirkin and R. L. Letsinger, *Science*, 2000, **289**, 1757–1760.
13 F. Patolsky, A. Lichtenstein and I. Willner, *Angew. Chem., Int. Ed.*, 2000, **39**, 940–943.
14 D. Gerion, F. Q. Chen, B. Kannan, A. H. Fu, W. J. Parak, D. J. Chen, A. Majumdar and A. P. Alivisatos, *Anal. Chem.*, 2003, **75**, 4766–4772.
15 Y. Weizmann, F. Patolsky and I. Willner, *Analyst*, 2001, **126**, 1502–1504.
16 S. Chen and R. W. Murray, *J. Phys. Chem. B*, 1999, **103**, 9996–10000.

